Identification and characterization of rod-derived cone viability factor.

Thierry Léveillard, Saddek Mohand-Saïd, Olivier Lorentz, David Hicks, Anne-Claire Fintz, Emmanuelle Clérin, Nükhet Cavusoglu, Frédéric Chalmel, Pascal Dollé, Olivier Poch, et al.

ROD-DERIVED CONE VIABILITY FACTOR IS A CLUE FOR THERAPY OF RETINITIS PIGMENTOSA

Thierry Léveillard[1†‡], Saddek Mohand-Saïd[1], Olivier Lorentz[1], David Hicks[1], Anne-Claire Fintz[1], Emmanuelle Clérin[1], Nükhet Cavusoglu[1], Frédéric Chalmel[2], Pascal Dollé[2], Olivier Poch[2], George Lambrou[3] and José-Alain Sahel[1,4†]

Address:

[1] Laboratoire de Physiopathologie Cellulaire et Moléculaire et de la Rétine, Inserm U592, Université Pierre et Marie Curie, Hôpital St-Antoine, 184 rue du Faubourg St-Antoine, 75571, Paris cedex 12, France

[2] Institut de Génétique et de Biologie Moléculaire et Cellulaire, 1 rue Laurent Fries, 67404 Illkirch, France

[3] Novartis Pharma AG Ophthalmology Research WKL-127.1.04 CH-4002 Basel, Switzerland

[4] Institute of Ophthalmology, University College of London, UK

† : These authors contributed equally to the work

‡ : Corresponding author: leveilla@st-antoine.inserm.fr

Running title: RdCVF

Retinitis Pigmentosa (RP) is an untreatable inherited retinal disease leading to blindness. The disease initiates with the loss of night vision due to rod photoreceptor degeneration, followed by irreversible progressive loss of cone photoreceptors death, [1,2,3,4]. Cone loss is responsible for the major visual handicap as cones are essential for day and high acuity vision[5]. Their loss is indirect since most RP genes are not expressed by these cells. We have previously shown that factors secreted from rods are an essential requirement for cone viability.[8,9,10,11]. We now have identified one such trophic factor by expression cloning and named it rod-derived cone viability factor (RdCVF). RdCVF is a novel truncated thioredoxin-like protein specifically expressed by photoreceptors. The identification of this protein offers new therapeutical possibilities for RP.

For expression cloning, a viability assay based on cone-enriched primary cultures form chicken embryos[12] was used. In contrast to mammals, bird retinas are cone-dominated. Indeed, they represent 60 to 80 % of the total population in cultured cells[11]. Once cultured, these cells degenerate over a few days. The addition of conditioned medium from wild-type mouse retinal explants delays this loss[11]. We thus performed a screen to isolate factors able to support cone survival.

A cDNA expression library was constructed from neural retinas of five-week-old wild-type mice. Plasmid DNA was purified from pools of 100 individual clones then used to transfect COS-1 cells. Conditioned medium (CM) from transfected COS cells was added to chicken retinal cultures seeded in 96-well plates. After 7 days of culture, an automated viability assay was performed (Live/Dead assay, Molecular probes, Eugene OR, USA). Twenty-one hundred pools, corresponding to 210,000 individual clones, were screened. Pool number 939 contained twice as many living cells as the negative controls (Fig. 1). By limiting dilution clone 939.09.08 was isolated and shown to contain a 502-bp insert with an open

reading frame encoding a putative 109-amino acid polypeptide. We named this gene rod-derived cone viability factor (RdCVF[13], Fig 2).

RdCVF was then expressed and purified as a fusion protein with gluthatione-S-transferase (Fig. 3a). Cone-enriched cultures were incubated with increasing amounts of GST-RdCVF or GST alone. Importantly, the addition of 10 µg/ml of purified GST-RdCVF doubled the number of living cells per plate. The rescue activity of this factor increases with higher protein concentration (Fig. 3b).

Next, retinal explants from five-week–old *rd1* mice (lacking rods) were co-cultured for 7 days with COS cells transfected with RdCVF cDNA (clone 939.09.08). Cone cells were labelled with cone-specific peanut agglutinin (PNA) and counted using stereological methods[10]. The number of cones per field was higher in retinal explants incubated with cells transfected with RdCVF than in controls (Fig. 3c). The amplitude of the rescue effect was 40% when compared to the number of cones loss during the one week period, a range of efficacy similar to what observed when wild-type retinas were used as a source of RdCVF activity[10]. RdCVF was thus able to slow down cone degeneration in both chick and mouse models[11].

We next tested the ability of RdCVF antibodies to block the endogenous activity. CM was prepared from five-week-old wild-type mouse retinal explants and immunodepleted with anti-RdCVF or control antibodies. Five-week-old *rd1* retinal explants (lacking rods) were incubated for seven days with CM and then the cones were labelled and counted. The number of cones was higher when *rd1* explants were incubated with CM preincubeted with control polyclonal antibodies than when they were incubated with medium alone (Fig. 3d, row 2 versus 1). The CM failed to stimulate cone survival in *rd1* explants when RdCVF was

specifically removed by immunodepletion (row 3). These results demonstrate that RdCVF is required for cone rescue in cultured explants.

To assess *in vivo* RdCVF effect, we injected 1 µl (100 ng) of the purified GST-RdCVF in the subretinal space of 35-day-old *rd1* mice, then repeated the injection 7 days after. The mice were sacrificed when seven week old (Fig 3e). The average of cones per mm^2 in animals injected with the RdCVF fusion protein (4500) is higher than in animals injected with either GST alone (3800) or with PBS (3500). The injection of RdCVF is thus able to prevent 40% of cones from degeneration in the *rd1* mouse over a period of two weeks.

Northern blotting analysis detected two distinct RdCVF mRNAs of 2.3 and 2.7 kb only in the retina and not in any other tissue tested (Fig. 4a). The pattern of RdCVF mRNA expression by real-time RT-PCR matched that of rhodopsin, largely increasing during maturation of photoreceptors in the wild-type mouse. However, in the *rd1* mouse, rod degeneration, as indicated by decreased rhodopsin mRNA levels, was accompanied by a dramatic decrease in RdCVF expression (Fig. 4b). The RdCVF gene is expressed as two mRNAs, most likely by alternative splicing. When tested by real-time RT-PCR, the most abundant mRNA encodes the factor that we have isolated (Fig 4c). The level of expression of RdCVF in the whole retina as well as in the photoreceptor layer (isolated by sectioning the mouse retina with a vibratome[14]) were similar. This suggests that RdCVF expression is mainly restricted to the outer nuclear layer containing the rods and cones (Fig. 4d). RdCVF is also expressed in cultures of pure photoreceptors (Fig. 4e).

Polyclonal antibodies raised against two specific regions of the RdCVF sequence (αRdCVF-N and –C, underlined in figure 2a) detected the same two bands (17 and 34 kDa, Fig 5a). *In vitro,* translated RdCVF consists only of a 17-kDa band possibly resulting from post-translational modifications of the 12 kDa polypeptide (Fig 3a). The amount of RdCVF

protein was similar in retinal extracts from normal and mutant strains at one week of age, prior to rod degeneration (Fig 5b). The levels of both bands were not substantially modified between two and five weeks of age in the wild-type mouse. In contrast, the amounts of RdCVF decreased from two weeks onwards in the *rd1* mouse, in correlation with the kinetics of rod degeneration[6]. The 34-kDa form of RdCVF was detected in the conditioned media produced from wild-type retinal explants (Fig 5c). Additional polyclonal antibodies were raised against a peptide specific to RdCVFL, the longer form of the protein (αRdCVFL). When transfected into Cos Cells, RdCVFL cDNA was specifically detected by αRdCVFL and αRdCVF-C antibodies, while the short form of RdCVF was specifically detected by αRdCVF-C antibodies (Fig. 5d). This demonstrates that the 34 kDa band detected in retinal extracts and CM corresponds to the long form of RdCVF.

Immunohistochemistry was performed on retinal sections from five-week-old mice with both the N- and C-terminal specific RdCVF antibodies (Fig. 6). Specific staining was observed on photoreceptor outer segments and/or on the interphotoreceptor matrix (Fig. 6c,g). Staining was particularly intense in discrete structures within the subretinal space, co-localizing with the binding of peanut agglutinin (PNA), a marker of cone matrix sheaths (Fig. 6a,d,e,h). No expression was detected in retinal sections from five-week-old *rd1* mice (result not shown). The preferential localization of RdCVF in the cone extracellular matrix suggests that a cell surface RdCVF receptor is present on target cells (Fig. 6c,g). As expected, RdCVF mRNA was prominently detected by in situ hybridization within the outer nuclear layer of the wild-type retina (Fig. 6i). The observed labelling is consistent with RdCVF being expressed by all rod photoreceptors. A Pax6 probe was used in the same experiment as a specificity control (Fig. 6j).

This study provides a biochemical basis for the previously described paracrine interaction between rod and cone photoreceptors that appears to play a key role in maintaining cone cell viability[10]. Previous studies suggested that Müller glial cells mediated photoreceptor rescue[15]. The finding that RdCVF is expressed predominantly by photoreceptors implies a new mode of trophic interactions. The systematic expression cloning strategy used here led to the identification of a protein from a family that has not previously been documented to include trophic factors.

RdCVF shows 33% similarity with thioredoxin[16] (Fig 2b). The C-terminus of RdCVF interrupts the thioredoxin motif and unlike other members of the thioredoxin family[16], recombinant RdCVF did not display detectable oxidoreductase activity[17] (result not shown). RdCVF is thus a truncated thioredoxin-like protein[16]. The founder member of this family, Trx-1 has also been isolated as the adult T-cell leukemia-derived factor[18], a factor secreted by cells by a mechanism that does not involve a signal peptide sequence, a signal also absent in RdCVF[19]. An alternatively spliced form of RdCVF is encoding a longer protein with a C-terminal extension and could have oxidoreductase activity (mouse RdCVF Long, Fig. 2b). RdCVF might be a new example of a bifunctional protein[20], with one extracellular form involved in cone viability, whereas the variant with an extended C-terminal sequence carries oxidoreductase activity.

Cone photoreceptors could be directly rescued by delivering RdCVF, either by means of gene or gene-based cell therapy. This provides hope for a therapeutic strategy aimed at preserving the remaining cones in RP patients. The implications of RdCVF are far-reaching, as it may be broadly effective in most RP types resulting from rod-specific mutations and even in the late stages of the disease. Visual function in patients with macular disease remains

stable as long as more than 50% of the cones are functional and is still substantial even when 90% of the cones have been lost[21]. As stated by Alan Wright "preserving cones would prevent 1.5 million people worldwide from becoming blind, since in an age of artificial lighting we can perfectly live without rods" [22].

Methods:

Animals:

Care and handling of mice in these studies conformed to the Association for Research an Vision and Ophthalmology Resolution on the use of animals in research.

Expression cloning:

A directional cDNA plasmid library was constructed using the neural retina mRNAs of 35-day-old wild-type (C57BL/6@N) mice. Pools of 100 plasmids were purified and used to transfect COS-1 cells[23]. The serum was removed and 48 hours after transfection, the conditioned medium from COS-transfected cells was harvested and incubated for 7 days with primary retina cultures from chicken embryos[12] (stage 29) in 96-well black tissue culture plates (Corning, Acton, MA, USA). Fourteen negative control wells (conditioned media from COS cells transfected with pcDNA3 vector alone) were included. A live/dead assay (Molecular Probes, Eugene, OR, USA) was used to monitor cell viability. For acquisition and cell counting, an algorithm based on the Metamorph software (Universal Imaging Corporation, West Chester, USA) was developed. Plates were read under an inverted fluorescence microscope (TE 200, Nikon) equipped with a mercury epifluorescent lamp with two excitation filters (485 and 520 nm), two emission filters (520 and 635 nm), a 10x objective, a computer-driven motorized scanning stage (Märzhäuser, Wetzlar, Germany) and a CCD camera (Fig. 1). For the first round of screening, numbers of live cells were compared to the mean number of live cells in the negative controls. For the second and third rounds, screening for sub-pools included positive controls (conditioned medium from wild-type retina).

RdCVF activity on cones of *rd1* retinal explants was tested by transfecting COS cells with pcDNA-RdCVF or the empty vector. COS-transfected cells were incubated for 72 hours in co-culture chambers containing retinal explants from 35-day-old *rd1* mice. The transfection

and co-culture steps were repeated for an additional 72 hours. For in vivo injections, 100 ng of purified GST-RdCVF and unfused GST was injected into the subretinal space of 35-day-old *rd1* mice. Cones were labelled with PNA (50 µg/ml) and counted by a stereological method[17].

DNA sequencing and data mining:

Isolated cDNAs were sequenced using the T7 primer. DNA sequences were used to screen databases using the Basic Local Alignment Search Tool (BLAST)[24].

Northern blotting and real-time RT-PCR:

For northern blotting analysis, 2 µg of poly-A mRNA was used. cDNAs were produced by random priming and normalized according to glucose-6-phosphate dehydrogenase mRNA. First strand cDNA (0.2 µl) was amplified in triplicate using 2 µM of the specific primers: 5'-TCTATGTGTCCCAGG-ACCCTACAG-3'; 5'-TTTATGCACAATAGTACCA-GGACAG-3' for RdCVF and 5'-TACAGAGGAGCAACAGGACCTCTTCCTCAGG-3'; 5'-TTAAGTACCACAACCGCTGGCAGTTGACG-3' for the long form on a lightcycler (Roche, Basel, Switzerland). Results are expressed as fold difference compared to the lowest expressing sample.

Recombinant protein production and purification:

The open reading frame of RdCVF was cloned into pGex2TK (Amersham, Uppsala, Sweden), and the fusion protein produced at 30°C in *E. coli* BL21 pLysS (Promega, Madison, WI, USA) and purified using standard procedures.

***In vitro* translation:**

pcDNA-RdCVF (2 µg) was incubated with TNT reticulocyte lysate (Promega, Madison, WI, USA) and ^{35}S methionine under standard procedures.

Polyclonal antibody production and purification:

Rabbit polyclonal antibodies were prepared with the following peptides (αRdCVF-N: IRNNSDQDEVETEAELSRRLEN); (αRdCVF-N: SQDPTEEQQDLFLRDMPE) and (αRdCVFL: RKYRVDRDVGRERGRNGRD). Immunoglobulins were purified from immune serum and specific antibodies were further affinity-purified onto immobilized epitopes. Polyclonal antibodies against blue cone pigment were produced using peptide (CGPDWYTVGTKYRSE) and purified as described above.

Western blotting, immunohistochemistry, in situ hybridization and immunodepletion:

For western blotting, 40 µg of whole cell extract from neural retina or conditioned medium from mouse retinal explants was resolved by 15% SDS-PAGE and transferred onto nitrocellulose. The membrane was saturated, and incubated for 3 hours at 20°C with affinity-purified anti-RdCVF polyclonal antibodies (0.1 µg/ml).

For immunohistochemistry, eyes were dissected from five-week-old wild-type mice (C57BL/6@N), fixed in 4% paraformaldehyde in PBS at 4°C for 12 hours, cryoprotected and embedded in OCT. Serial cryostat sections (10 µm) were cut. Coverslips and slides were rinsed in PBS and blocked with blocking buffer (PBS containing 0.1% Tween 20 and 0.1% BSA) for 30 minutes, then incubated with the diluted RdCVF antibodies (2 µg/ml) overnight at 4°C. The slides were rinsed in PBS (ten washes over a total of 1 hr) and incubated with anti-goat IgG-AlexaFluor 488™ (Molecular Probes, Eugene, OR, USA). Slides were finally washed extensively in PBS and mounted in PermaSave. Cellular distribution was observed by use of confocal laser scanning microscopy (Zeiss LSM 510 v2.5) scanning device mounted on a Zeiss Axiovert 100 inverted microscope.

For immunodepletion, retinal explants from 35-day-old wild-type (C57BL/6@N) neural retina were maintained for 48 hours at 37°C in a 5% CO_2 atmosphere in a chemically defined medium[12] (1 explant/0.75 ml). Affinity-purified polyclonal antibodies (2.5 mg) were covalently coupled to Sepharose beads via protein A. Six milliliters of conditioned medium

were incubated overnight at 4°C with immobilized polyclonal antibodies, control antibodies raised against the blue cone visual pigment and αRdCVF-C antibodies. The retinal explants prepared from 35–day-old mice were incubated over a period of 7 days with conditioned media. Cones were labelled with PNA. Labelled explants were mounted on glass slides and placed on a computer-driven motorized scanning stage (Märzhäuser, Wetzlar, Germany). Cone cells were counted by use of a specially designed procedure using Metamorph software (Universal Imaging Corporation, West Chester, USA). Briefly, a composite image of the explants was generated to calculate the explant area. Within this area, five images at the focal depth for x40 magnification after excitation at 520 nm and emission at 635 nm were acquired with automatic exposure times. These stacks of images were deconvoluted in order to count cone numbers within the depth of the explants. The automation gives a density of cones that is reproducibly lower by a factor of 2 than the stereological methods due to the filtering of the images. In situ hybridization was performed on cryosections of eyes from five-week-old wild-type mice (C57BL/6@N) essentially as described[24], using dixoxigenin-UTP (Roche) labelled riboprobes.

Enzymatic assay:

Assays were performed according to Holmgren[17]. The enzymatic activity of *E. coli* thioredoxin was monitored as a positive control.

Statistical analysis:

Statistical analysis of the results is based on different non parametric tests. Mann Witney t test for paired comparisons and Bon Ferroni method for multiple comparisons[26]. Variance analysis (ANOVA) and Fischer t test were used to analyse the dose-response effect.

Acknowledgments:

The authors thank Aurélie Gluck, Juliette Ravey, Danièle Thiersé, Manuel Simonutti, Valérie Forster, Noëlle Hanotteau, Emmanuelle Clérin, Géraldinbe Millet-Puel, Géraldine Lucchi, Pascal Oberlin and Georges Tarlet for excellent technical assistance. The authors thank Arno Dolemeyer (Novartis-Pharma, Basel, Switzerland), Christophe Grolleau (Roper Scientific, Evry, France) and Eugène Scherbeck (Couvoirs de l'Est, Wilgottheim, France) for their invaluable help. The authors thank Pierre Chambon for constant support.

This work was financed by Novartis, Inserm, Ministère de la Recherche, the Association Française contre les Myopathies (AFM), the Fédération des Aveugles de France, Retina France, Foundation Fighting Blindness (USA), IPSEN foundation, and the European Community (PRO-AGE-RET program). The authors thank Emiliana Borelli, Antoine Triller, Valérie Heidinger and Olivier Goureau for critical reading of the manuscript.

References:

1. http://www.sph.uth.tmc.edu/Retnet/ [2003]

2. Rosenfeld, P.J. *et al.* A null mutation in the rhodopsin gene causes rod photoreceptor dysfunction and autosomal recessive retinitis pigmentosa. *Nat Genet* **1**, 209-213. (1992).

3. McLaughlin, M.E., Sandberg, M.A., Berson, E.L. & Dryja, TP. Recessive mutations in the gene encoding the beta-subunit of rod phosphodiesterase in patients with retinitis pigmentosa. *Nat Gene.* **4**, 130-134. (1993).

4. Kajiwara, K., Berson, E.L. & Dryja, T.P. Digenic retinitis pigmentosa due to mutations at the unlinked peripherin/RDS and ROM1 loci. *Science* **264**, 1604-1608. (1994).

5. Dowling, J.E. The retina: An approachable part of the brain, Harvard Press, Cambridge MA. (1987).

6. Carter-Dawson, L.D., La Vail, M.M. & Sidman, R.L. Differential effect of the rd mutation on rods and cones in the mouse retina. *Invest Ophthalmol Vis Sci*, **17**, 489-498. (1978).

7. Pittler, S.J., Keeler, C.E., Sidman, R.L. & Baehr, W. PCR analysis of DNA from 70-year-old sections of rodless retina demonstrates identity with the mouse rd defect. *Proc Natl Acad Sci U S A.* **90**, 9616-9619 (1993).

8. Mohand-Saïd, S. *et al.* Photoreceptor transplants increase host cone survival in the retinal degeneration (rd) mouse. *Ophthalmic Res* **29**, 290-297. (1997).

9. Mohand-Saïd, S., Hicks, D., Léveillard, T., Dreyfus, H. & Sahel, J. Selective transplantation of rods delays cone loss in a retinitis pigmentosa model. *Arch Ophthalmol*, **118**, 807-811. (2000).

10. Mohand-Saïd, S. *et al.* Normal rod photoreceptors increase cone survival in the retinal degeneration (rd) mouse. *Proc Natl Acad Sci USA*, **95**, 8357-8362. (1998).

11. Fintz, A.C. *et al.* Partial characterization of retina-derived cone neuroprotection in two culture models of photoreceptor degeneration. *Invest Ophthalmol Vis Sci* **44**, 818-825. (2003).

12. Adler, R. & Hatlee, M. Plasticity and differentiation of embryonic retinal cells after terminal mitosis. *Science* **243**, 391-393. (1989).

13. Disease associated protein, international patent # PCT/EP 02/03810

14. Fontaine, V., Kinkl, N., Sahel, J., Dreyfus, H. & Hicks, D. Survival of purified rat photoreceptors *in vitro* is stimulated directly by fibroblast growth factor-2. *J Neurosci* **18**, 9662-9672. (1998).

15. Zack, D. Neurotrophic rescue of photoreceptors: are Müller cells the mediator of survival? *Neuron* **26**, 285-286. (2000).

16. Arner, E.S. & Holmgren, A. Physiological functions of thioredoxin and thioredoxin reductase. *Eur J Biochem* **267**, 6102-6109. (2000).

17. Holmgren, A. Thioredoxin catalyzes the reduction of insulin disulfides by dithiothreitol and dihydrolipoamide. *J Biol Chem*, **254**, 9627-9632 (1979).

18. Wakasugi, N. *et al.* Adult T-cell leukemia-derived factor/thioredoxin, produced by both human T-lymphotropic virus type I- and Epstein-Barr virus-transformed lymphocytes, acts as an autocrine growth factor and synergizes with interleukin 1 and interleukin 2. *Proc Natl Acad Sci U S A* **87**, 8282-8286. (1990).

19. Nickel, W. The mystery of nonclassical protein secretion. A current view on cargo proteins and potential export routes. *Eur J Biochem*. **270**, 2109-2119 (2003).

20. Jefferey, C.J. Moonlighting proteins. *Trends Biochem* **24**, 8-11. (1999).

21. Geller, A.M. & Sieving, P.A. Assessment of foveal cone photoreceptors in Stargardt's macular dystrophy using a small dot detection task. *Vision Res* **33**, 1509-1524. (1993).

22. Wright, A.F. A searchlight through the fog. *Nat Genet*, **17**, 132-134. (1997).

23. Chen, C. & Okayama, H. High-efficiency transformation of mammalian cells by plasmid DNA. *Mol Cell Biol* 7, 2745-2752. (1987).

24. Altschul, S.F. *et al.* Gapped BLAST and PSI-BLAST: a new generation of protein database search programs. *Nucleic Acids Res.*, **25**, 3389-402. (1997).

25. Cau E., Gradwohl G., Fode C. & Guillemot F. Mash1 activates a cascade of bHLH regulators in olfactory neuron progenitors. *Development*, **124**, 1611-1621. (1997).

26. Dixon, W.J. & Massey Jr, F.J. in Introduction to statistical analysis. Mc Graw-Hill, New York. (1969).

27. Plewniak, F. *et al.* PipeAlign : a new toolkit for protein family analysis. *Nucleic Acids Res.*, **31**, 3829-3832. (2003).

Figure legends:

Figure 1: Schematic representation of the expression cloning strategy.

Figure 2: a, RdCVF nucleotide and deduced amino acid sequences. The polypeptide sequences used to generate the polyclonal antibodies directed against the N and C terminal regions are underlined. ↕ indicates a potential N-glycosylation site. **b,** Multiple alignment of the RdCVF sequences (see Discussion) from mouse and human origin with the *Escherichia coli* Thioredoxin and human Thioredoxin ATL-derived factor (Trx-1). The secondary structural elements of the Trx-1 structure (PDB code: 1ert) are shown above the alignment. Sequence conservations are indicated: white with black shading and white with grey shading for identical residues in all sequences or in 80% of the sequences, respectively; black with grey shading for conserved residues in 80% sequences according to the following physicochemical proximity (P,G,A,S,T); (F,Y,W); (I,L,M,V); (D,E,Q,N); (R,K,H); (C). Gaps are indicated by dashes. Alignment was done with PipeAlign[27] and subsequently corrected manually based on secondary structural elements.

Figure 3: a, Gel analysis of purified GST (lane 1), GST-RdCVF (lane 2) and thrombin-cleaved and purified RdCVF (lane 3). Arrows on the left point to the RdCVF proteins, white arrowhead points to GST. Molecular weight markers are shown on the right. **b**, Activity of 5 and 15 µg/ml of GST (1 and 3 respectively) and 5 and 10 µg/ml of GST-RdCVF (lanes 2 and 4 respectively) on chicken cone-enriched cultures. The assay represents the sum of eight independent experiments. **c**, Activity of RdCVF cDNA transfected into COS-1 cells on cone viability in *rd1* mouse retinal explants. pcDNA3 (C, lane 1), pcDNA-RdCVF (lane 2). **d,** Immunodepletion with anti-RdCVF-C antibodies. Chemically defined medium (C, lane 1), Conditioned medium from wild-type retinal explants after immunodepletion with control

antibodies (α-control, lane 2), after immunodepletion with RdCVF antibodies (α-RdCVF-C, lane 3). **e,** Subretinal injection of 1 µl of PBS (C, lane 1), GST (100ng, lane 2) and GST-RdCVF (100ng, lane 3).

Figure 4: Expression of RdCVF mRNA. Panel **a**, Northern blotting analysis of RdCVF mRNA prepared from different adult mouse tissues. Kidney (lane 1), *rd1* retina (2), wild-type retina (3), testis (4), spleen (5), intestine (6), lung (7) and cerebellum (8). **b**, real-time RT-PCR analysis quantifying RdCVF levels in wild-type (1,3,5) and *rd1* (2,4,6) retina at post-natal day (PN) 8 (1,2), 15 (3,4) and 35 (5,6) days after birth. The results are expressed as a fold difference compared to the level expressed in 35–day-old *rd1* mice. **c,** real-time RT-PCR analysis quantifying RdCVF (lane 1) and RdCVF-Long (lane 2). **d,** RT-PCR products of RdCVF mRNA amplification from wild type retina (lane 1) and isolated photoreceptors (PR, lane 2). **e**, RdCVF mRNA expression: negative control (C, lane 1) , 5 weeks wild type retina (lane 2) and in pure culture of PR (lane 3) and Müller glial cells (Mü, lane 4).

Figure 5: Production of RdCVF protein. **a,** Western blotting of retinal extracts from wild-type mice. *In vitro* translated RdCVF (1), retinal extract probed with αRdCVF-N (2) and αRdCVF-C (3) antibodies. **b,** Western blotting using αRdCVF-C polyclonal antibodies from retinal extracts from wild-type and *rd1* mice at 8 (1,5), 15 (2,6), 21 (3,7) and 35 (4,8) days after birth from wild type (1-4) and *rd1* (5-8) retinas. Wild-type whole brain, 35 days after birth (9). **c,** Western blotting analysis with N terminal RdCVF antibodies of wild-type retinal explants (1), conditioned media from wild-type (2) and *rd1* (3) mice 35 days after birth. **d**, Cos-1 cell extracts after transfection of cDNA encoding the open reading frame of RdCVF and RdCVFL. The control correspond the empty vector. The extracts were probed by western blotting with αRdCVF-C and αRdCVFL specific antibodies.

Figure 6: Immunolabelling of 35-day-old wild-type mouse retina. **a,e,** PNA labelling. **b**,**f**, Nomarski image of immunolabelled sections. **c,g**, Staining with an affinity-purified polyclonal anti-RdCVF antibody. N terminal (b) and C terminal (g). Merging of PNA and RdCVF staining. **i,j**, In situ hybridization of RdCVF (i) and Pax6 (j) riboprobes on adjacent sections of 5 week-old wild-type mouse retina. gc : ganglion cells ; inl : inner nuclear layer ; onl : outer nuclear layer.

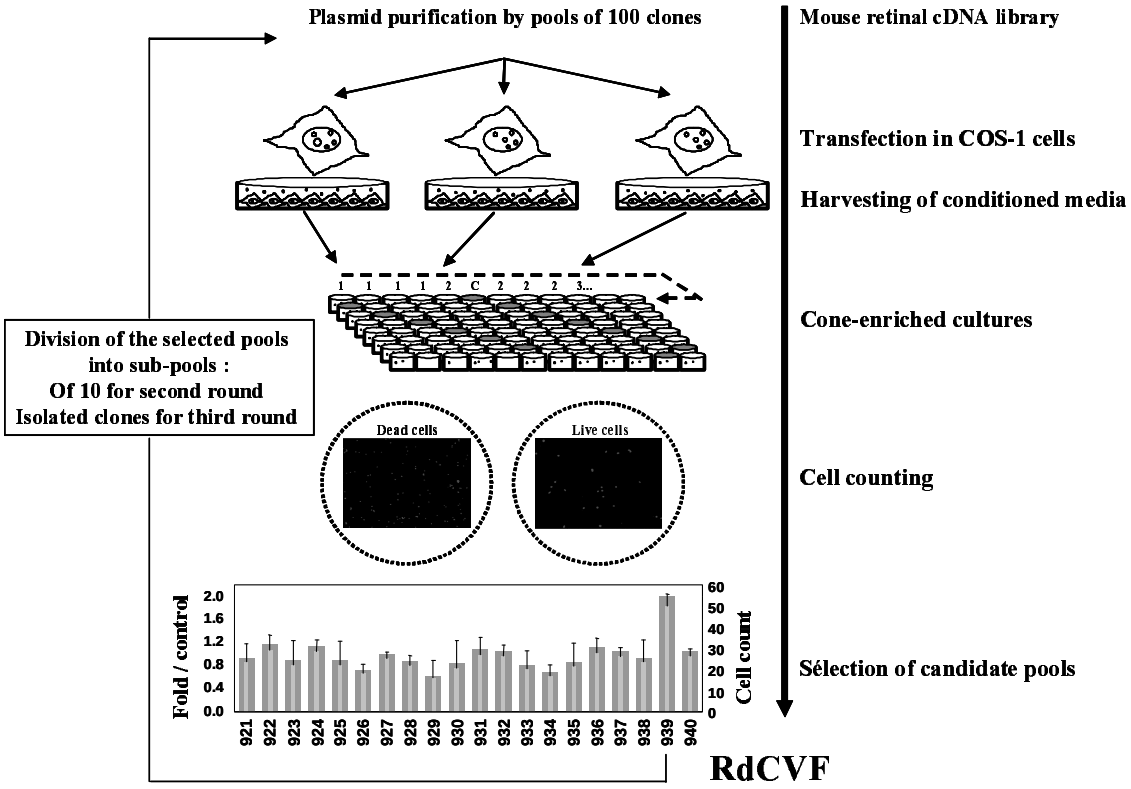
Plasmid purification by pools of 100 clones
Mouse retinal cDNA library
Transfection in COS-1 cells
Harvesting of conditioned media
1 1 1 1 2 C 2 2 2 3...
Cone-enriched cultures
Division of the selected pools into sub-pools :
Of 10 for second round
Isolated clones for third round
Dead cells
Live cells
Cell counting
Fold / control
Cell count
2.0
1.6
1.2
0.8
0.4
0.0
60
50
40
30
20
10
0
921 922 923 924 925 926 927 928 929 930 931 932 933 934 935 936 937 938 939 940
Sélection of candidate pools
RdCVF

Figure 1

a

```
GAATTCCGTTGCTGTCGGCAGGCTCCAGGCCACATCGGATCCCTCTCTGGGTCCCCAGCT   60

CCTTGCATACTGCTACCATGGCATCTCTCTTCTCTGGACGCATCTTGATCAGGAACAACA  120
                M  A  S  L  F  S  G  R  I  L  I  R  N  N  S
                                              ↕
GCGACCAGGATGAAGTGGAGACAGAGGCAGAGCTGAGCCGTAGGTTAGAGAATCGTCTGG  180
  D  Q  D  E  V  E  T  E  A  E  L  S  R  R  L  E  N  R  L  V

TGTTGCTGTTCTTCGGCGCCGGCGCCTGTCCCCAGTGCCAGGCCTTTGCCCCAGTCCTCA  240
  L  L  F  F  G  A  G  A  C  P  Q  C  Q  A  F  A  P  V  L  K

AAGACTTCTTCGTGCGGCTCACTGACGAGTTCTACGTGCTGCGGGCAGCACAGCTGGCCC  300
  D  F  F  V  R  L  T  D  E  F  Y  V  L  R  A  A  Q  L  A  L

TGGTCTATGTGTCCCAGGACCCTACAGAGGAGCAACAGGACCTCTTCCTCAGGGACATGC  360
  V  Y  V  S  Q  D  P  T  E  E  Q  Q  D  L  F  L  R  D  M  P

CTGAAAAATGGCTCTTCCTGCCGTTCCATGATGAACTGAGGAGGTGAGGCCCCAGGGAAG  420
  E  K  W  L  F  L  P  F  H  D  E  L  R  R  *

ACCAGGGAGGGCTTCCTGGAGAAGGCATTTCCCTGGAGGTTTACTGTCCTGGTACTACTT  480

GTGCATAAAGAGGTATTCCTC                                         502
```

b

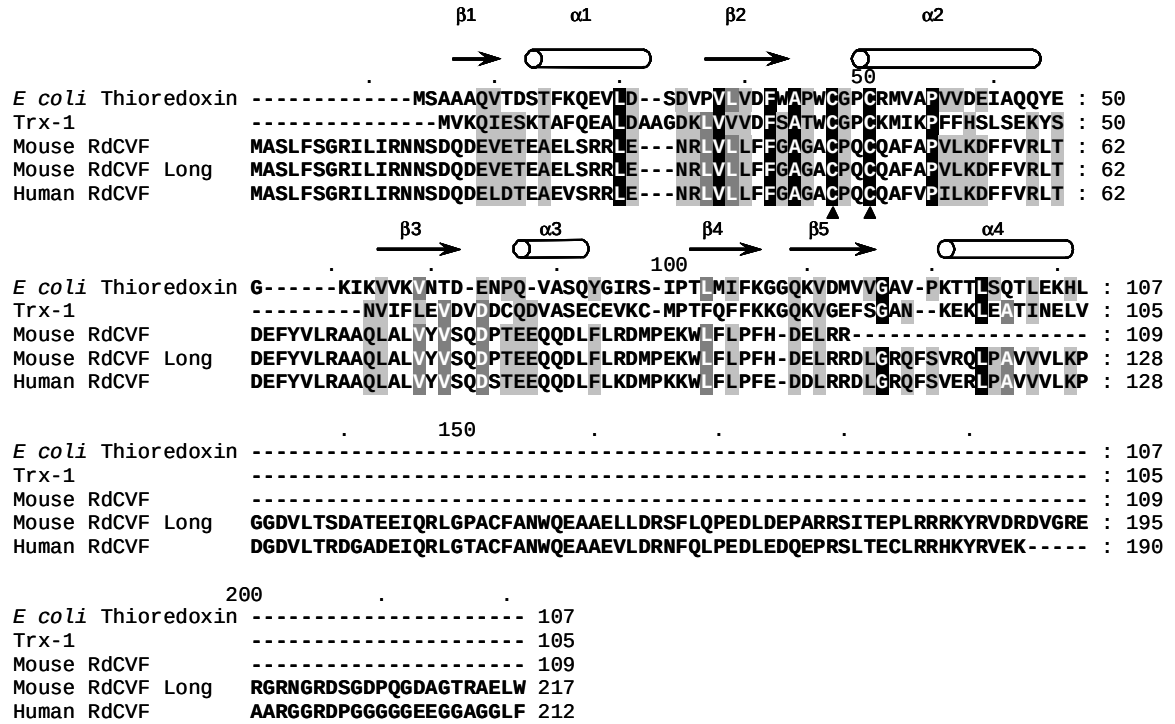

Figure 2

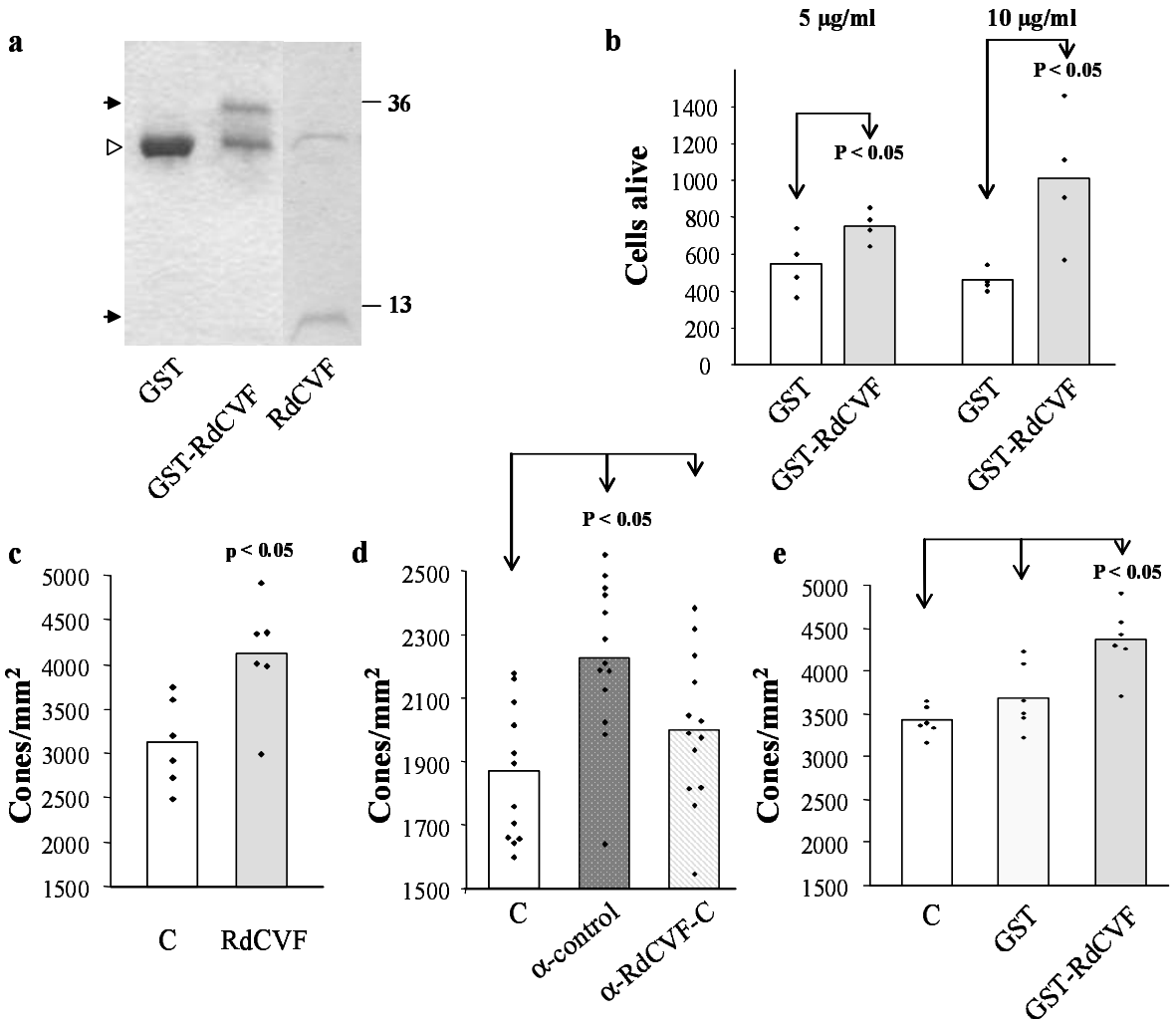
a
36
13
GST
GST-RdCVF
RdCVF
b
5 µg/ml
10 µg/ml
P < 0.05
P < 0.05
P < 0.05
Cells alive
1400
1200
1000
800
600
400
200
0
GST
GST-RdCVF
GST
GST-RdCVF
c
p < 0.05
Cones/mm2
5000
4500
4000
3500
3000
2500
2000
1500
C
RdCVF
d
P < 0.05
Cones/mm2
2500
2300
2100
1900
1700
1500
C
α-control
α-RdCVF-C
e
P < 0.05
Cones/mm2
5000
4500
4000
3500
3000
2500
2000
1500
C
GST
GST-RdCVF

Figure 3

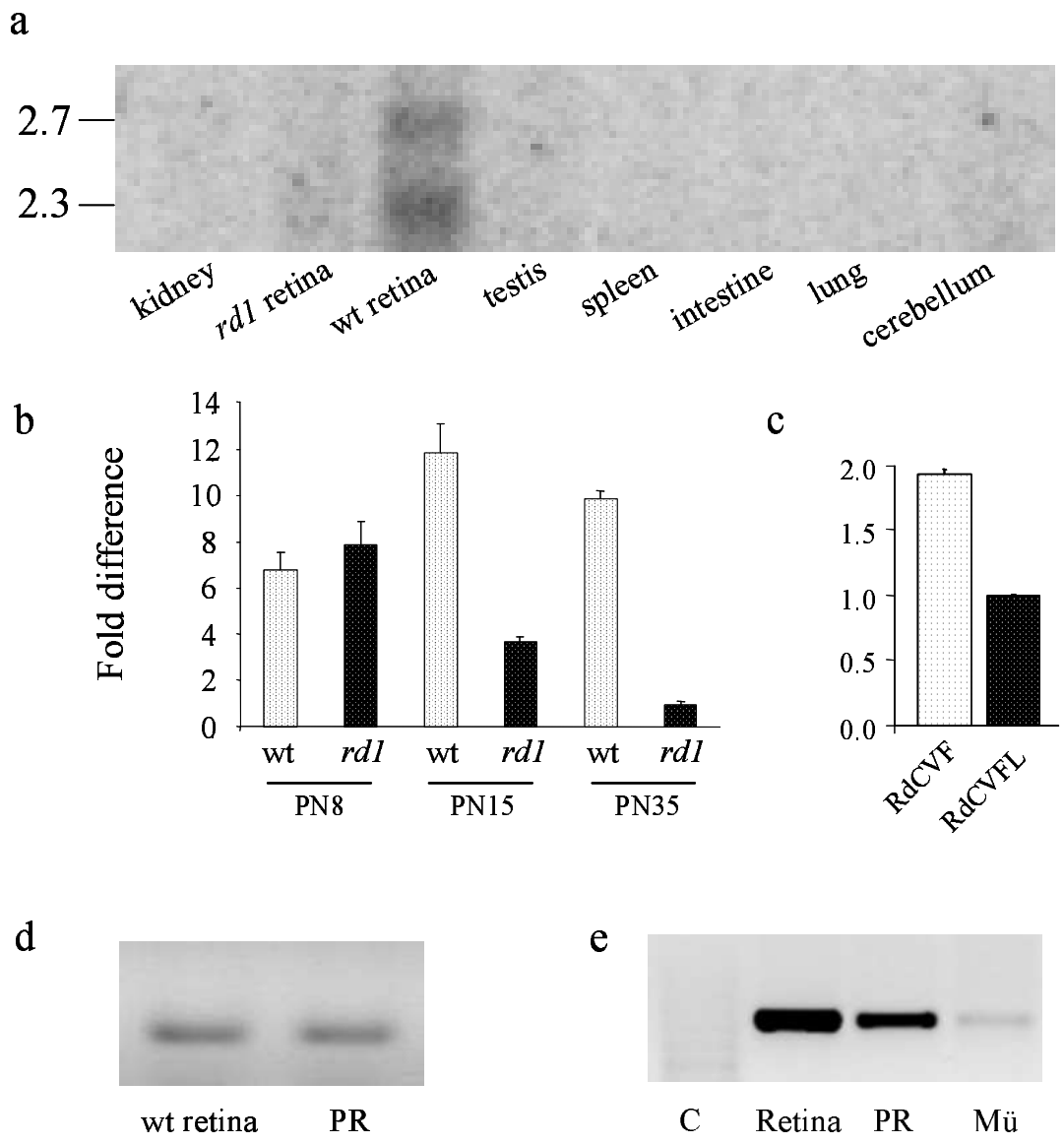
a
2.7
2.3
kidney
rd1 retina
wt retina
testis
spleen
intestine
lung
cerebellum
b
Fold difference
14
12
10
8
6
4
2
0
wt
rd1
wt
rd1
wt
rd1
PN8
PN15
PN35
c
2.0
1.5
1.0
0.5
0.0
RdCVF
RdCVFL
d
wt retina
PR
e
C
Retina
PR
Mü

Figure 4

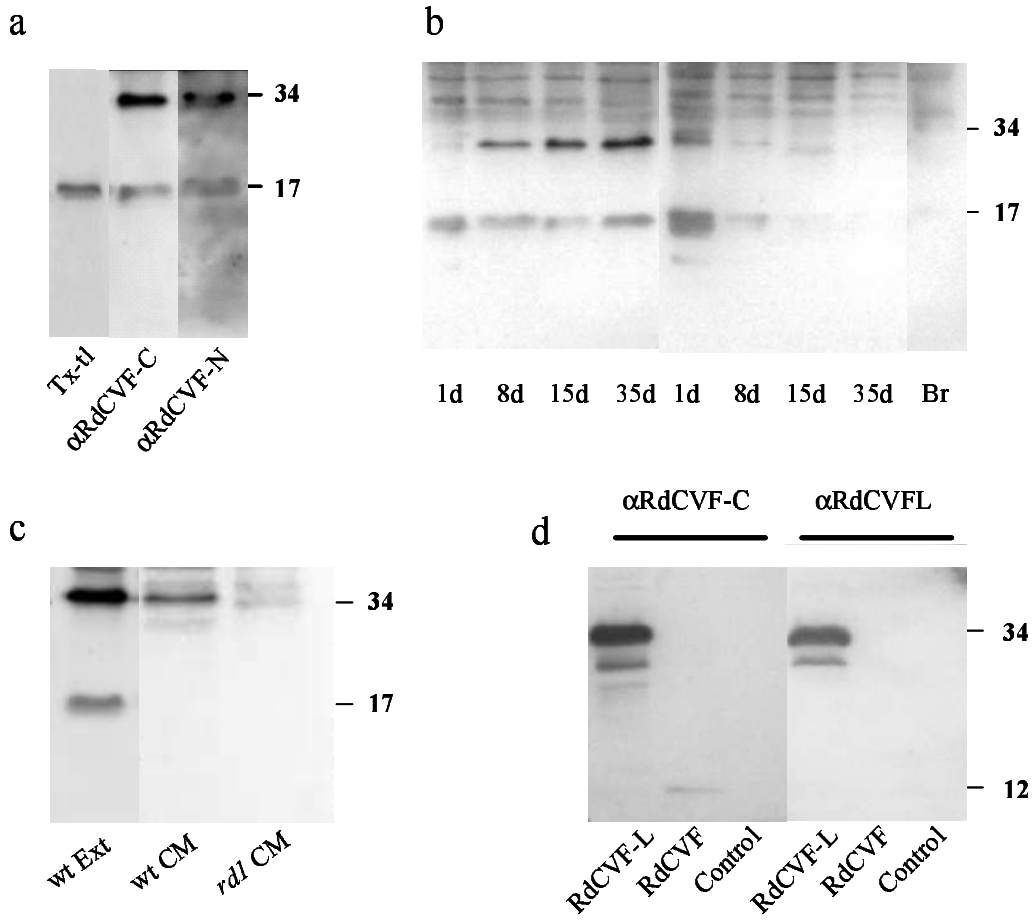
a
34
17
Tx-tl
αRdCVF-C
αRdCVF-N
b
34
17
1d
8d
15d
35d
1d
8d
15d
35d
Br
c
34
17
wt Ext
wt CM
rdl CM
d
αRdCVF-C
αRdCVFL
34
12
RdCVF-L
RdCVF
Control
RdCVF-L
RdCVF
Control

Figure 5

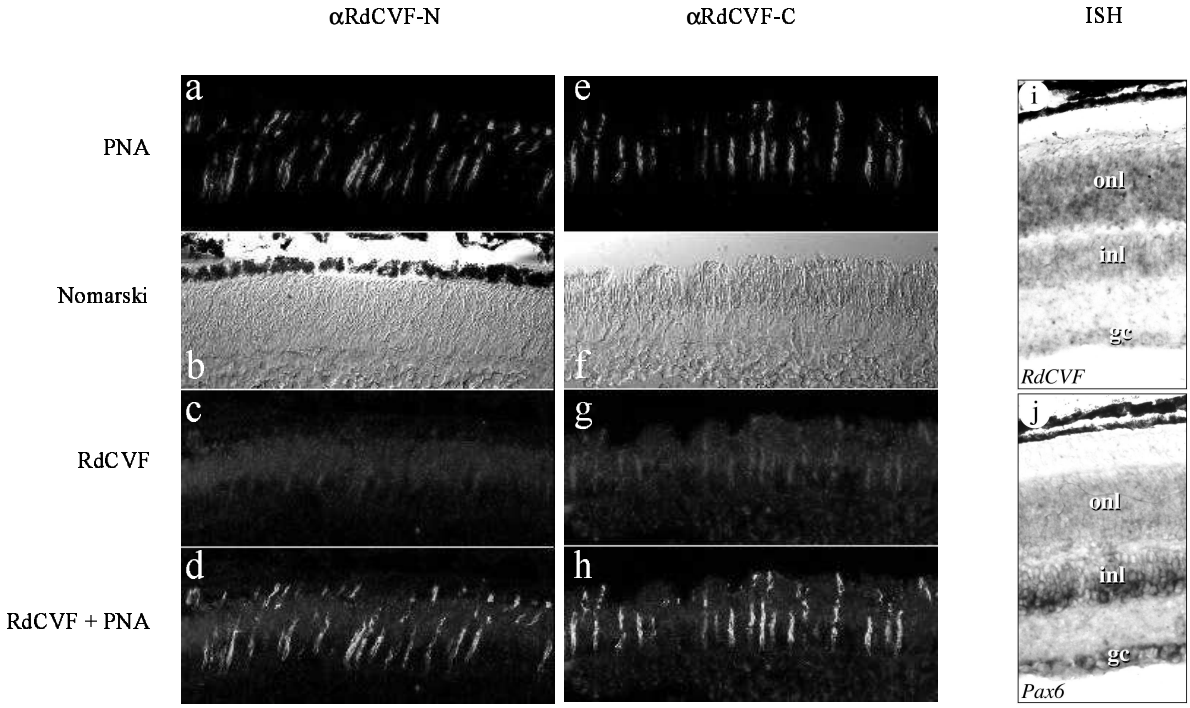
αRdCVF-N
αRdCVF-C
ISH
PNA
Nomarski
RdCVF
RdCVF + PNA
a
b
c
d
e
f
g
h
i
onl
inl
gc
RdCVF
j
onl
inl
gc
Pax6

Figure 6